

Application of boron doped diamond for electro-Fenton and photoelectro-Fenton decolorization of azo dye from dye-containing wastewater: Acid Red 1

Rui Wang^{1,2,*}, Jiashun Cao¹, Junsong Song³, Jiajia Liu², Yifei Zhang²

¹ College of Environment, Hohai University, Nanjing, 210098, China

² Environmental Engineering College, Nanjing Polytechnic Institute, Nanjing, 210048, China

³ College of Life and Health, Nanjing Polytechnic Institute, Nanjing, 210048, China

*E-mail: wangruijsnj@163.com

Received: 6 November 2021 / Accepted: 13 December 2021 / Published: 5 January 2022

This work was focused on the study and application of boron-doped diamond (BDD)/air-diffusion cell for the decolorization of Acid Red 1 (AR1) as an azo dye using electro-Fenton (EF) and photoelectro-Fenton (PEF) as electrochemical advanced oxidation techniques. The experiments were conducted on treatment of 100ml of 300 mg/l AR1 solution in 0.05M Na₂SO₄ at pH 3.0 with 0.50mM Fe²⁺ under an applied current density of 16.6 to 66.6 mA/cm². The results indicated that the better performance of the PEF method for color removal at 33.3mA/cm² after 12 minutes of electrolysis revealed 96.7% of discoloration in the PEF method and 95.2% of discoloration in the EF technique. The evolution of carboxylic acids (oxalic (OXL) and oxamic (OXM) acids) as degraded AR1 products by EF and PEF was also examined using HPLC. Results showed that the carboxylic acids were accumulated and destroyed by generated hydroxyl radicals. Because of the slow reaction of BDD (•OH) with Fe(III)–oxalate and Fe(III)–oxamate complexes, carboxylic acids were reduced to a final concentration of 35.9 mg/l and 0.7 mg/l after 240 minutes. The evolution of SO₄²⁻ and NH₄⁺ as released inorganic ions during azo dye degradation was determined by ion chromatography, and results showed that the released SO₄²⁻ and NH₄⁺ were completely released, accumulated and decay by intermediates and reached to 98.2 mg/l and 42.5 mg/l for EF, and 98.2 mg/l and 6.5 mg/l for PEF at 240 minutes, respectively. The results demonstrated that the EF system was able to generate and accumulate a sufficient amount of H₂O₂ to adequately treat AR1 solution by EF and PEF, and the higher rate of mineralization in PEF was related to a synergistic effect in the generation of free radicals to destroy organic dyes and UVA light. Therefore, these findings show that the PEF technique is the most effective treatment method to quickly destroy and mineralize azo dye-contaminated wastewater.

Keywords: Azo dye; Acid Red 1; Decolorization; Boron-doped diamond; azo dye-contaminated wastewater; Electro-Fenton; Photoelectro-Fenton

1. INTRODUCTION

Azo dyes are organic compounds and refer to a class of synthetic dyes composed of nitrogen as the azo —N=N— functional group or chromophore in their molecular structures [1]. These organic compounds are mainly produced in developing nations such as China, India, Korea and Argentina. These dyes are the most commonly used group of dyes in the textile industry [2, 3]. Moreover, these are extensively used in printing, paper manufacturing, cosmetics, leather, fiber, paint, and food industries. These organic compounds not only possess coloring functions but also show antimicrobial activity [4].

Azo dyes based on benzidine and aromatic amine are classified as carcinogenic and cause several types of human and animal tumors, birth defects, or other reproductive harm [5]. A research has shown that exposure to azo dyes increases bladder cancer risk [6]. Some azo dyes degrade under reductive conditions and have the potential to release aromatic amines [7]. The carcinogenic activation mechanisms for azo dyes such as production of toxic amines and oxidation of azo dyes with structures containing free aromatic amine groups result in the formation of bio-recalcitrant natural toxics that are dangerous to humans as well as other animals [8, 9]. Therefore, the European Commission has adopted a proposal to restrict the use of dyes containing aromatic amines, as well as azo dyes.

Accordingly, many studies have been performed for the determination and degradation of the azo dyes from the industrial wastewater through photocatalytic treatment [10], electrochemical oxidation [11], EF and PEF treatments [12-15] and anaerobic-aerobic sequential processes [16, 17]. Among these methods, EF and PEF treatments as fast, efficient and cost-effective techniques are the most environmentally friendly processes for the degradation of organic pollutants and pharmaceuticals [18].

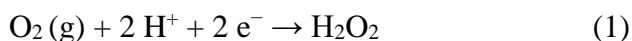
Acid Red 1 (AR1; disodium;5-acetamido-4-hydroxy-3-phenyldiazenylnaphthalene-2,7-disulfonate) as an aryl azo naphthol compound is directly used in the wool–polyamide fibre and textile Printing [19-21]. It can be utilized in the leather and cosmetics industries, and it can also be employed to make the color amyllum and ink. These extensive applications of AR1 in industries result in its presence in natural water resources and getting into drinking water from natural sources. Therefore, this study was conducted in the application of BDD for EF and PEF decolorization of Acid Red 1.

2. MATERIALS AND METHODS

2.1. Electrochemical measurements

A cylindrical electrochemical cell was used for EF experiments which opened and undivided a 150 ml Pirex® glass cell vessel (DOT Scientific Inc., USA) with a double jacket that circulated water to keep the solution at a constant temperature. Carbon-polytetrafluoroethylene air-diffusion (GDE) as cathode (PTFE, geometric area of 3 cm^2 , E-TEK, Somerset, NJ, USA) and BDD (geometric area of 3 cm^2 , Adamant Technologies SA, La Chaux-de-Fonds, Switzerland) as anode were utilized in the electrochemical cell. Before the electrochemical measurements, a polarization in a $0.05\text{ M Na}_2\text{SO}_4$ (99%, Merck, Germany) solution at 150 mA/cm^2 for 3 hours allowed the cleaning and simultaneous activation of the anode and cathode. The distance between the electrodes was 2 cm. The outer face of

the cathode was in contact with the solution which was fed with air pumped at a rate of 500 ml/min for continuous production of H₂O₂ as the following electrochemical reaction based on reduction of oxygen [22]:



The treatment process was accomplished at a current density range from 16.6 to 66.6 mA/cm², which was supplied by a DC power supply (HP 6552A, Agilent, USA), a The dye aqueous solution was introduced at a concentration of 300 mg/l in the reservoir and recirculated at a flow rate of 0.2 ml/h using a plant centrifuge pump (1/3 HP Electric Pump, Vektek, USA). The pH was adjusted to the same initial pH (pH 3.0) by the addition of H₂SO₄ (97%, Merck, Germany). The 0.5mM Fe²⁺ (FeSO₄·7H₂O, ≥99.0%, Sigma-Aldrich) as catalyst was added to the solution before starting the electrolysis. The EF process was accomplished in a 4-hour reaction, and the treated solutions were continuously stirred with a magnetic bar at a stirring speed of 750 rpm. For the photoelectro-Fenton process under UVA irradiation, a fluorescent black light blue lamp (TL/6 W/08, λ range 320–400 nm with λ_{max} = 360 nm, Philips) located at 6 cm above the solution was used, yielding a photoionization energy of 5 W/m², which was determined with a UVA radiometer (CUV 5 from Kipp & Zonen, The Netherlands).

2.2. Characterizations

At room temperature, UV-Vis spectrophotometry (UV-Vis 1800, Shimadzu, Kyoto, Japan) was used for determination the H₂O₂ concentration at light absorption of the titanic-hydrogen peroxide complex at λ = 408 nm [23]. During the oxidation reactions, aliquots of samples were regularly withdrawn for analysis, neutralized at pH 8 to quench the action of produced oxidants, and the samples were filtered through PTFE (0.45 μm, Thomas Scientific, New Jersey, USA) membrane filters. A color removal rate evaluation was performed using UV-Vis spectroscopy at 478 nm. The TOC of the solutions was immediately measured by injecting 50 μL samples into the TOC analyzer (VCSN, Shimadzu, Kyoto, Japan) that an accuracy of ±1% was obtained by any injections in the analyzer. The concentration of produced carboxylic acids was determined by reversed-phase HPLC coupled to a photodiode array detector set at λ = 212 nm.

The ion-exclusion high performance liquid chromatography (HPLC; 600 Waters Pharmaceutical Division, Milford, MA, USA) was used for the evaluation of the generated carboxylic acids which consists of a photodiode array detector (DAD; 996 Waters, Milford, MA, USA) at λ = 210 nm and was equipped with a Aminex HPX-87H column (BIO-RAD, Hercules, 300 × 7.8 mm, 9 μm, CA, USA). The column temperature was 35°C, the mobile phase consisted of 4mM H₂SO₄ and the flow rate was 0.6 ml/min. For quantification of the produced inorganic nitrogen ions, the ionic chromatography with LC coupled to a Shimadzu CDD 10Avp conductivity detector was applied. The NH₄⁺ content was determined in 25 mM boric acid (≥99.0%, Sigma-Aldrich), 4.5 mM tartaric acid (≥99.5%, Sigma-Aldrich), 1.5 mM 18-crown-6 (99.0%, Sigma-Aldrich) and 2.0 mM 2,6-

pyridinedicarboxylic (99.0%, Sigma-Aldrich) solution at 1.0 ml/min as mobile phase [24]. The NO_3^- and SO_4^{2-} concentrations were evaluated with circulating a mobile phase composed of 2.5 mM phthalic acid (997%, Merck, Germany) and 2.5mM tris(hydroxymethyl)aminomethane ($\geq 99.0\%$, Sigma-Aldrich) at 1.5 ml/min [24].

The equation (2) was used to calculate the percentage of dye removal (removal efficiency) based on color absorbance at 478 nm [25]:

$$\text{Decolourization (\%)} = \frac{C_0 - C}{C_0} \times 100 \quad (2)$$

Where C_0 and C (mg/l) denote the concentrations of dye before and after adsorption. TOC values were used for calculating the amount of mineralization current efficiency (MCE) according to the equation (3) [26]:

$$\text{MCE (\%)} = \frac{(\Delta\text{TOC}) e^{nFVs}}{4.32 \times 10^7 \text{ mlt}} \times 100 \quad (3)$$

where $(\Delta\text{TOC})_{\text{exp}}$ denotes the TOC decay (mg/l) at time t (hour), F is the Faraday constant (96487 C/mol), V corresponds to the treated solution volume (L), 4.32×10^7 is a conversion factor to homogenize units ($600 \text{ s/h} \times 12000 \text{ mg C/mol}$), I is the applied current (A), m is the number of carbon atoms in the molecule (16 carbon atoms in this case). n is number of electrons that consumed the total mineralization of each molecule (84) required for the theoretical total mineralization of its anion form was taken as the following reaction [24]:



2.4. Preparation the dye wastewaters

For studying the applicability of the PEF method for treatment of real samples, the wastewater from textile industrials (South China's Guangdong Province) was provided, and utilized for the preparation of the 0.05 M Na_2SO_4 pH 3.0. Five different dyes were added to the wastewater to ensure the presence of dye contaminants in the wastewater, containing AR1, Acid Red 18 (AR18), Allura Red AC (ARAC), Ponceau 4R (P4R) and 1,10-phenanthroline-ferrous chelate (PFC). All the dye is provided in analytical grade from Sigma-Aldrich. AR18, ARAC, P4R and PFC have the maximum absorption wavelength of 505-508 nm [27-29].

3. RESULTS AND DISCUSSION

3.1. UV-vis absorption spectra

The removal of azo dye by anodic oxidation with the electrogenerated H_2O_2 (AO- H_2O_2), EF and PEF in the 150 ml cell was studied by electrolyzing 300 mg L^{-1} of the AR1 in 0.05 M Na_2SO_4 at pH 3.0, at a current density of 33.3 mA/cm^2 and $35 \text{ }^\circ\text{C}$, with the addition of 0.5 mM Fe^{2+} for the electrochemical advanced oxidation processes. As observed from Figure 1, the UV-vis spectra of the

initial dye solution diluted 1:6 depicts a weak shoulder at 420 nm and maximum absorption at 482 nm which is characteristic of AR1 [30], and is attributed to an equilibrium with of the two tautomeric forms of azo dyes, including azo and hydrazone forms. The azo-hydrazone tautomeric form contains hydroxyl groups and involves the hydrogen bonding with an azo group [31]. Accordingly, a maximum visible wavelength of 508 nm was used for the decolorization of AR1 by the EF and PEF processes.

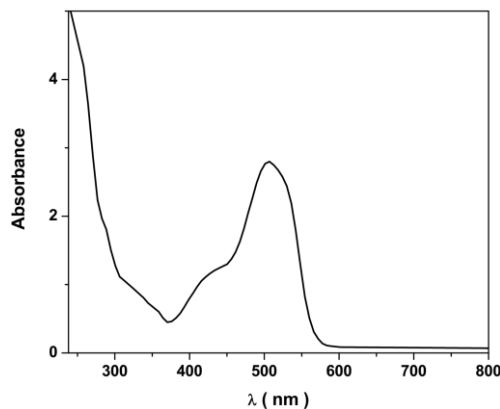
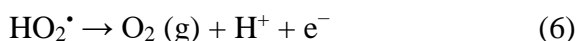
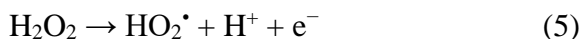


Figure 1. UV–vis absorption spectra of the initial AR1 solution diluted 1:6.

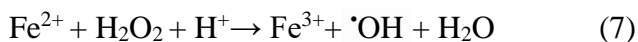
3.2. Decolorization of the AR1 solution under EF and PEF processes

The current density is an important variable in electrochemical advanced oxidation processes due to its ability to regulate the generated oxidants such as $\cdot\text{OH}$ and BDD($\cdot\text{OH}$) [32]. Studies have been shown that the treatment has been performed based on the capability of H_2O_2 accumulation in the BDD/GDE cell, correlating with the electrogenerated H_2O_2 and anodic oxidation (AO- H_2O_2) [33]. When the H_2O_2 concentration reaches a steady state which corresponds to the production rate from reaction (1) is equal to the rate of its destruction via reactions (5) and (6) that evidence of oxidation of the electrogenerated H_2O_2 to O_2 at the BDD anode with the generation of hydroperoxyl radical ($\text{HO}_2\cdot$) as a weak oxidant [34]:

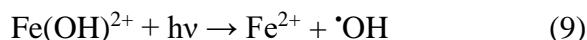


The current density effect was investigated for the degradation of a 300 mg/l AR1 solution in 0.05 M Na_2SO_4 at pH 3.0 through both EF and PEF treatments with 0.50 mM Fe^{2+} under applied current density from 16.6 to 66.6 mA/cm². Measurements showed that there was no remarkable change in pH value in treatment time up to 240 minutes, and the slight decrease in pH value from 3.0 to 2.9–2.95 in the treatment process is related to the generation of acidic products like carboxylic acids [35], it was continuously adjusted to its initial value (pH 3.0) through adding small amounts of 0.5 M NaOH. Furthermore, the AR1 and its conjugated products can react with the resulting BDD ($\cdot\text{OH}$), which is limited by their mass transfer to the anode, demonstrating that mass transfer controls the AO-

H₂O₂ process [36]. Results from Figure 2 show that the removal efficiency is increased with increasing current which is related to the enhancement of H₂O₂ concentration, and indicates the great effect of current density on the enhancement of the rate of electrochemical processes in reactions (1) and (5). Mainly, the efficiency of EF process depends on the concentration of Fe²⁺ due to the concentration of hydroxyl radical as the main oxidizing agent in the EF process. As a consequence, production of more oxidant •OH because of the faster cathodic formation of H₂O₂ leads to the acceleration of reaction (7), which results in large amounts of BDD(•OH) as a consequence of Fenton's reaction (8) [37].



Moreover, the addition of a small quantity of Fe²⁺ can increase the removal of H₂O₂ through the Fenton's reaction (7) to generate the powerful oxidizing agent of •OH [38]. As seen from Figure 2, 76.7% discoloration is observed for EF at 16.6 mA/cm² after 12 minutes of electrolysis which is enhanced to 81.7% under PEF. There is the better performance of PEF method for color removal at 33.3 mA/cm² after 12 minutes of electrolysis which indicated 96.7% of discoloration in PEF method and 95.2% of discoloration in the EF method. The slight acceleration to decomposition of H₂O₂ under light irradiation may be attributed to the increase the regeneration rate of Fe²⁺ from the photolysis of hydroxy complex Fe(OH)²⁺, and the main role of Fe(III) species at pH 3 in enhancement of Fenton's reactions (7) and (9) that it can produce more •HO through its photolysis [39].



The results demonstrate that the electro-Fenton system is able to generate and accumulate a sufficient amount of H₂O₂ to adequately treat a solution with 100 mg/l TOC of AR1 by EF and PEF.

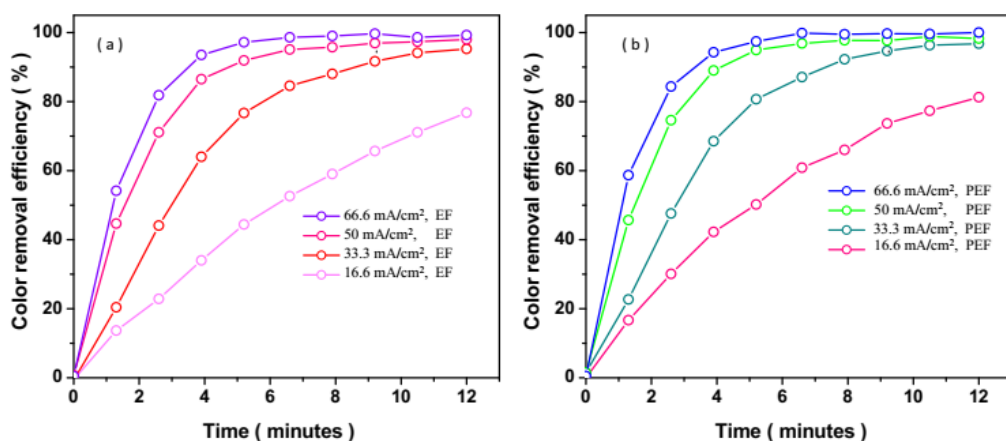
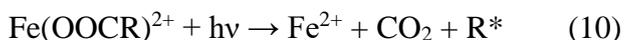


Figure 2. Effect of current density on removal efficiency of a 300 mg/l AR1 solution in 0.05M Na₂SO₄ of pH 3.0 at 35°C through (a) EF and (b) PEF treatments with 0.50 mM Fe²⁺ under applied current density from 16.6 to 66.6 mA/cm².

Table 1 shows the results of the analyses of the kinetic mechanisms of both processes by different kinetic equations and the result shows a good correlation with the pseudo-second-order kinetic model which is represented by the term of $\ln(C_0/C)$ versus time. The obtained pseudo-second-order rate constant well-known apparent discoloration rate constant (k_2), the correlation coefficient for linear regression (R^2) are summarized in Table 1. It reveals that an increase in the current leads to an almost linear increase in the k_2 value which is correlated with the reaction of $\cdot\text{OH}$, and overall reaction rate is limited by reactions (1) and (7) because of linear generation of H_2O_2 during the both of the EF and PEF treatments [40, 41].

3.3. Mineralization of AR1 solution

Degradation of the by-products generated during the reaction of AR1 and $\cdot\text{OH}$ can be evaluated by solution TOC degradation. Further measurements were carried out to determine the BDD($\cdot\text{OH}$), $\cdot\text{OH}$ and UVA light effect on treatment of 300 mg/l AR1 solution at 66.6 mA/cm² using AO-H₂O₂, EF and PEF methods. In AO-H₂O₂ method, no catalyst is added to the solution, and heterogeneous hydroxyl radicals (BDD($\cdot\text{OH}$)) and reactive oxygen species like $\text{HO}_2\cdot$ are formed by H₂O and H₂O₂ oxidation as equations (8) and (5), respectively [42]. Therefore, BDD($\cdot\text{OH}$) and $\text{HO}_2\cdot$ can destroy the organics, and the other reactive oxygen species like (H_2O_2) have a much smaller effect on organic destruction [43]. In EF process, Fe^{2+} is added to the solution, and hydroxyl radicals are formed through the reaction (7). BDD($\cdot\text{OH}$) and $\cdot\text{OH}$ as oxidizing agents react at the dyes and complexes of Fe(III) [44]. In the PEF process, as expected light irradiation can help effectively to degradation of organic pollutants by additional photo-oxidation because it accelerates regeneration Fe^{2+} from reaction (9) and photodecarboxylated of Fe(III)-carboxylate complexes according to the equation (10) [37]:



As seen from Figure 3, the solution is gradually removed by AO-H₂O₂, and 81.7% TOC removal is achieved in 240 minutes, illustrating the BDD($\cdot\text{OH}$) reaction with intermediates. In the EF process, 89.9% TOC removal is observed in 240 minutes. The mineralization is accelerated because of high oxidation efficiency of $\cdot\text{OH}$. As seen, TOC is mineralized by the PEF method up to 93.7% after 80 minutes, whereupon the rate of mineralization is very low due to formation of products that are slowly degraded mostly by the $\cdot\text{OH}$ created in the Fenton electrochemical cell as reaction (7) and in a smaller value by BDD($\cdot\text{OH}$) produced from reaction (8) [35]. So, 98.1% TOC reduction is attained only after 240 minutes of PEF treatment. The results show that the higher rate of mineralization in PEF related to a synergistic effect in more generation of free radicals to destroy organic dyes and UVA light where the radicals' contribution in the oxidation mechanism corresponds to dye elimination, and oxidation products are more quickly destroyed upon UVA light irradiation according to the reaction (10), and resulted to extra regeneration of Fe^{2+} in treatment system [45].

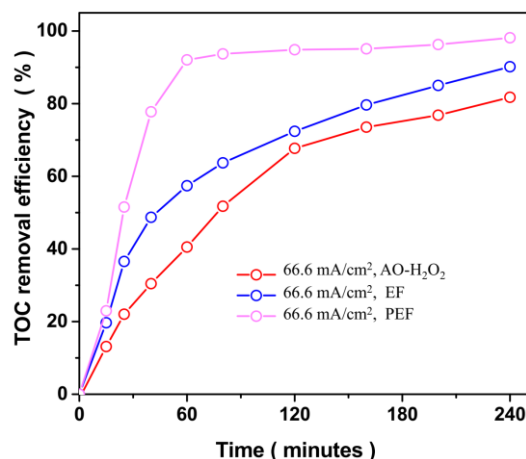


Figure 3. Removal efficiency of TOC for electrolysis of 150 ml of 300 mg/l AR1 solution using AO-H₂O₂, EF and PEF method at 66.6 mA/cm² in 0.05 M Na₂SO₄, pH 3.0 at 35 °C.

Moreover, the relative oxidation power of the electrochemical advanced oxidation processes was analyzed using a pseudo first-order kinetic model as given by Lagergren as following equation because of the exponential decay for the removal of TOC in Figure 3 [46]:

$$\ln(\text{TOC}/\text{TOC}_0) = -k_{\text{TOC}} t \quad (11)$$

Table 1 shows that the best fit is found for up to 80 minutes for PEF, as well as up to 80 minutes for both of EF and AO-H₂O₂. The obtained value for kinetic constant for TOC removal as an apparent rate constant for TOC removal (k_{TOC}), slope and its R^2 are also presented in Table 1. It can be found that the k_{TOC} values in 66.6 mA/cm² of PEF is 3.3-fold higher than EF and 4.9-fold higher than AO-H₂O₂, corroborating the synergistic effect of $\cdot\text{OH}$ and UVA light on the degradation process of organic pollutants [47]. The similar behavior is also observed for MCE in Figure 4 so that the MCE slowly mineralized from 26.0% at 15 minutes to 8.4% at 240 minutes under AO-H₂O₂ process, whereas the higher removal rate is observed for EF process from 36.0% to 9.0% from 15 to 240 minutes. In PEF process, the MCE value is dropped from 45.7% at 40 minutes to 27.7% at 80 minutes, and reaches 10.2% at 240 minutes. In all processes, Figure 4 highlights a drastic decrease of MCE value with prolonging electrolysis which is associated with the continuous loss of organic matter and the generation of more recalcitrant by-products which rarely reacted by BDD($\cdot\text{OH}$) and $\cdot\text{OH}$ [48]. In the PEF process, this observation is more pertinent when the treatment time is more than 80 minutes because of the very low rate of TOC reduction to complete mineralization.

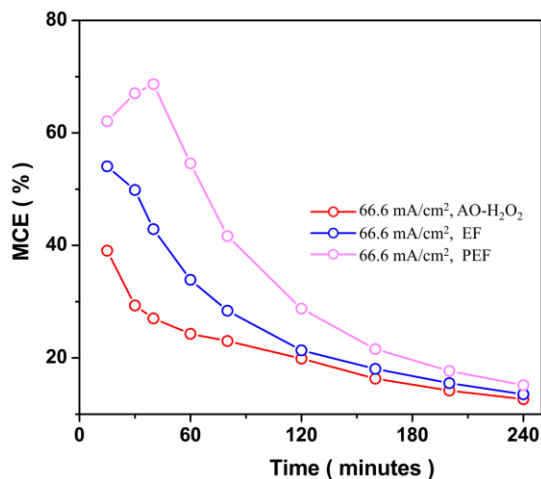


Figure 4. Evolution of MCE for electrolysis of 150 ml of 300 mg/l AR1 solution using AO-H₂O₂, EF and PEF method at 66.6 mA/cm² in 0.05 M Na₂SO₄, pH 3.0 at 35 °C.

Table 1. Apparent discoloration rate constant and kinetic constant for TOC removal achieved for the decolorization of 150 ml of 300 mg/l AR1 in 0.05 M Na₂SO₄ of pH 3.0 using AO-H₂O₂, EF and PEF methods.

Method	Condition	Current density (mA/cm ²)	K _{TOC} × 10 ³ (min ⁻¹)	R ²	K ₂ (min ⁻¹)	R ²
AO-H ₂ O ₂		66.6	8.55	0.9973	Not determined	Not determined
EF	0.5 mM Fe ²⁺	16.6	7.65	0.9955	0.1215	0.9959
		33.3	9.45	0.9973	0.285	0.9968
		50	10.8	0.9961	0.525	0.9942
		66.6	12.6	0.9978	0.645	0.9988
PEF	0.5 mM Fe ²⁺ , Under 6 W/cm ² UVA irradiation	16.6	No good linear correlation	No good linear correlation	0.141	0.9979
		33.3	31.5	0.9968	0.315	0.9998
		50	36	0.9966	0.525	0.9972
		66.6	42	0.9977	0.645	0.9968

Figures 5a and 5b show the results of the study on the effect of applied current density from 16.6 to 50 mA/cm² on the oxidation/mineralization efficiency of EF and PEF on the AR1 solution. It can be found that the TOC decay is gradually increased with increasing current density for EF, indicating 68%, 82%, 85.4% and 89.8% mineralization at 16.6, 33.3, 50 and 66.6 mA/cm² after 240 minutes, respectively, which is related to an increase in the rate of reactions (1), (7) and (8) and destruction of intermediates, as a consequence, more production of BDD(·OH) and ·OH. In PEF process, TOC is reduced by 92.5% and 93.6% after 160 minutes at 16.6 and 33.3 mA/cm², respectively, and 92.6% and 93.6% after 80 minutes at 50 and 66.6 mA/cm², respectively. The

generation of high recalcitrant products leads to prolonged electrolysis and hinders the complete mineralization of the solution. The TOC amounts after 240 minutes reach between 97.4% and 98.1%. The finding confirms the faster mineralization in PEF in all currents is attributed to photo-oxidation and the synergistic action of UVA irradiation and $\cdot\text{OH}$.

The calculated mineralization constant value (k_{TOC}) for these assays is also summarized in Table 1. As observed, there was no linear correlation for 16.6 mA/cm² of PEF which is related to its short activation time. For the EF, a four-fold increase in current density leads to only a 1.6-fold increase in the k_{TOC} , it means to loss of relative oxidation power of some oxidizing species ($\cdot\text{OH}$) [43]. In PEF, as two-fold increase in current value density leads to only a 1.3-fold increase in the k_{TOC} . Figures 6 show the calculated MCE values that confirm the above findings. Therefore, as expected in EF experiments, the highest value of MCE at 15 minutes decreased from 65.3% at 16.6 mA/cm² to 34.2% at 66.6 mA/cm² because of the consumption of the excess of created hydroxyl radicals by non-oxidizing waste reactions, the main loss of BDD($\cdot\text{OH}$) due to its oxidation to O₂ gas through reaction (12) [49, 50]. According to Moreover, BDD, as a strong oxidant, facilitates the formation of peroxodisulfate (S₂O₈²⁻) ions from the oxidation of SO₄²⁻ ions, which are weaker oxidants present in electrochemical cells, via reactions (13) and (14) [50]:



Figure 6 displays the greatest values for MCE between 91.8% at 16.6 mA/cm² and 44.7% at 66.6 mA/cm² in PEF process, which is much larger than those obtained in the EF case.

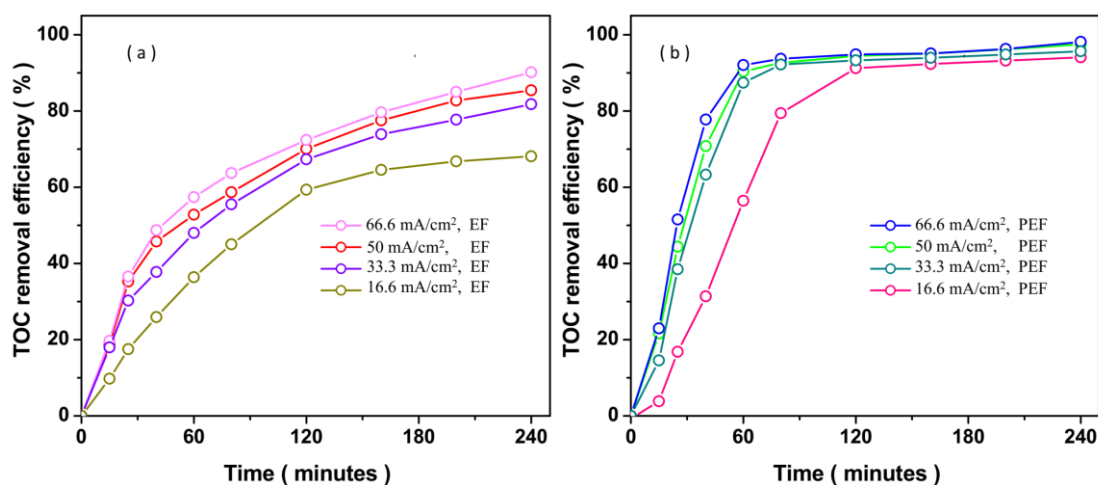


Figure 5. TOC removal efficiency vs. electrolysis time for removal 300 mg/l AR1 solution in 0.05 M Na₂SO₄ of pH 3.0 at 35 °C through (a) EF and (b) PEF treatments with 0.50 mM Fe²⁺ under applied current density from 16.6 to 66.6 mA/cm².

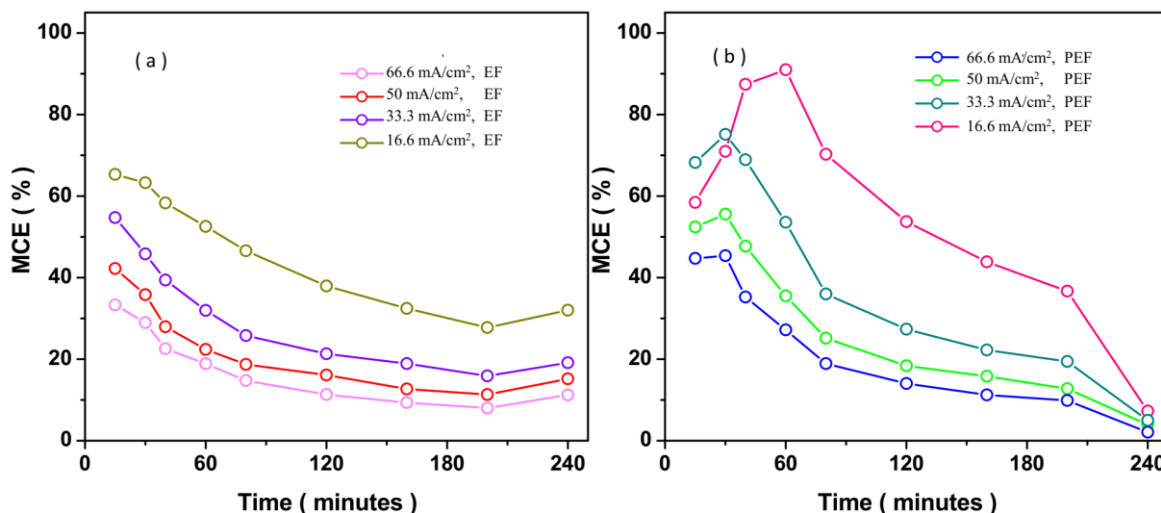


Figure 6. Evaluation MCE vs. electrolysis time for treatment of 300 mg/l AR1 solution in 0.05 M Na₂SO₄ of pH 3.0 at 35 °C through (a) EF and (b) PEF treatments with 0.50 mM Fe²⁺ under applied current density from 16.6 to 66.6 mA/cm².

The waste reactions (12–14) may also occur during the PEF process. In this process, the most persistent complexes as by-products under EF conditions can quickly photolysis by UVA light, which illustrates the higher oxidation ability of PEF [51]. Therefore, these findings show that the PEF process is a successful method to quickly destroy and mineralize dye-contaminated wastewater.

The degraded AR1 products by EF and PEF were also examined using HPLC. The peaks of OXL and OXM acids were identified at HPLC retention times of 7.0 min and 9.39 min, respectively. OXL and OXM acids are carboxylic acids and are directly oxidized to CO₂ [52]. OXL acid is expected to be formed from the cleavage of the aromatic rings of the azo dye. The breaking of aromatic moieties containing an NH₂ group could result in the formation of OXM acid [52].

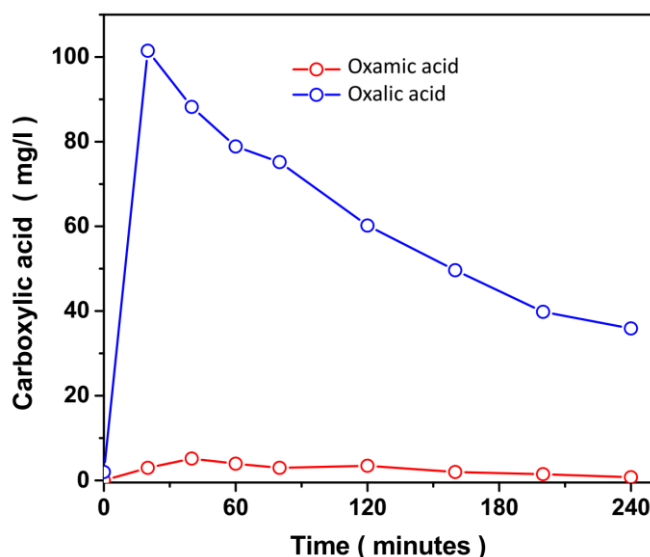


Figure 7. Evolution of detected carboxylic acids (OXL and OXM acid) content under EF process for treatment of 300 mg/l AR1 solution in 0.05 M Na₂SO₄ of pH 3.0 at 35°C at 33.3 mA/cm².

Figure 7 shows the evolution of detected carboxylic acids under the EF process at $33.3\text{mA}/\text{cm}^2$. As seen, OXL acid was quickly accumulated and attained its maximum content of 101.5 mg/L at 20 minutes, denoting that its Fe(III) complexes was rapidly destroyed by generated hydroxyl radicals [52]. The slow reaction of Fe(III)–oxalate complexes with BDD($\cdot\text{OH}$) leads to slow degradation for long period and it was reduced to a final amount of 35.9 mg/l at 240 minutes. OXM acid evolution reveals that it was formed in smaller value, with a maximum concentration of 5.1 mg/l at 40 minutes, and it was reduced to a final amount of $\sim 0.7\text{ mg/l}$ at 240 minutes because of to the slow reaction of Fe(III)-oxamate complexes with BDD($\cdot\text{OH}$) in EF [47].

The evolution of released inorganic ions during the EF and PEF processes for treatment of AR1 solution at $66.6\text{ mA}/\text{cm}^2$ was followed by ion chromatography. The conversion of the initial N (14.6 mg/L) and initial S atoms (33.33 mg/l) of the AR1 solution into NO_3^- and NH_4^+ ions, and SO_4^{2-} ions in PEF were identified by ionic chromatography, according to reaction (4). The NO_3^- ion was accumulated to a negligible value ($<0.1\text{mg/l}$). The results of the time-course record of the concentration of inorganic ions are displayed in Figure 8. As observed from Figure 8a, the initial S atoms as released SO_4^{2-} were completely released at 120 minutes and reached 90.1 mg/l for EF and 94.4 mg/l for PEF. Figure 8b exhibits a progressive accumulation of NH_4^+ ion with electrolysis time. In EF process, there is slow increase of NH_4^+ content with time to reach a 62.8 mg/l at 120 minutes. After that, it degrades to 42.5 mg/l at 240 minutes. Results of the PEF process show that NH_4^+ ion was quickly accumulated up to 50.7 mg/l at 40 minutes, and they decayed considerably, down to 6.5 mg/l at 240 minutes. Therefore, it can be suggested that the decay of NH_4^+ by intermediates under the PEF treatment, light irradiation can enhance the degradation rate of NH_4^+ by photoactivation and intermediates [53].

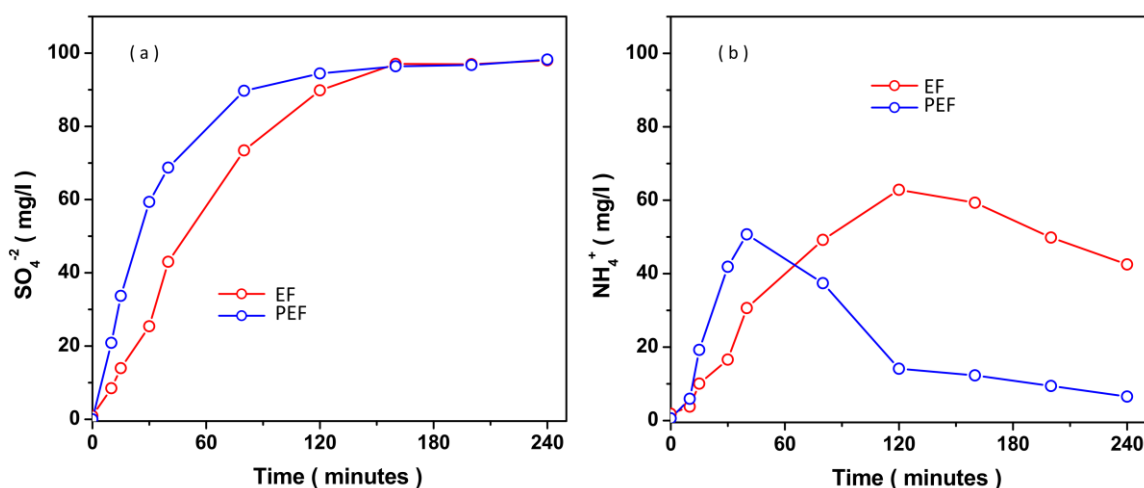


Figure 8. Time-course record of concentration of inorganic ions (a) SO_4^{2-} and (b) NH_4^+ under EF and PEF processes for degradation of 300 mg/l AR1 solution in $0.05\text{ M Na}_2\text{SO}_4$ of pH 3.0 at $35\text{ }^\circ\text{C}$ at $66.6\text{mA}/\text{cm}^2$

Table 2 exhibits the comparison between the obtained results of this study for treatment AR1

and other reported PEF treatments of dyes and organic compounds in BDD/GDE cells. As observed, by considering the initial concentration of dye, applied current density, power of UVA irradiation, and treatment time, the results of this study for treatment AR1 are acceptable and comparable with the other reported PEF treatments of dye and organic compounds.

Table 2. Comparison between the obtained results of this study with other reported PEF treatment of dyes and organic compounds 0.05 Na₂SO₄ and 0.5 mM Fe²⁺, pH 3.0 and 35 °C.

Compound	Content of Compound (mg/l)	Applied current (A)	UVA irradiation power (W/cm ²)	Time (minute)	TOC removal efficiency (%)	MCE (%)	Ref.
Acid Red 1	300	0.2	2	240	98.1	44.7	This work
Acid Yellow 36	108	0.5	300	360	95	65	[14]
Acid Red 29	244	0.050	2	180	98	28	[52]
Acid Red 88	50	1	300	360	98	20	[54]
Acid Yellow 9				360	95	20	
Orange-G	295	0.2	2	360	98	10	[53]
Disperse Red 1	100	1	300	240	97	82	[44]
Disperse Yellow 9				240	96	80	
Cresols	128	1	300	180	98	122	[55]
Enrofloxacin	158	1	300	300	86	42	[56]
Mecoprop	634	1	300	540	97	93	[13]

3.4. Applicability performance of PEF for rapid decolorization of dye-contaminated wastewater

Four dye-contaminated wastewaters were selected to evaluate the applicability of PEF under the identified optimal conditions (0.05 M Na₂SO₄ and 0.5 mM Fe²⁺, pH 3.0, 66.6 mA/cm², 35 °C and each dye concentration of 300mg/l) was studied for the decolorization of four more different dye and compound wastewaters (AR18, ARAC, P4R and PFC). Figure 9 shows that the decolorization efficiency after 240 minutes reaches about 99.99%, 98.24%, 98.98%, 99.00% and 97.74% for AR1, AR18, ARAC, P4R and PFC, respectively.

Decolorization and mineralization of the organic dyes are more difficult because of complex aromatic molecular structures that make them more stable. So, the TOC removal efficiency of AR1, AR18, ARAC, P4R and PFC reaches 98.12%, 87.94%, 85.11%, 75.65% and 89.82%, respectively. The results indicated that the BEF method can near-completely decolorize the selected dyes, and can be applied for the treatment of the textile wastewater.

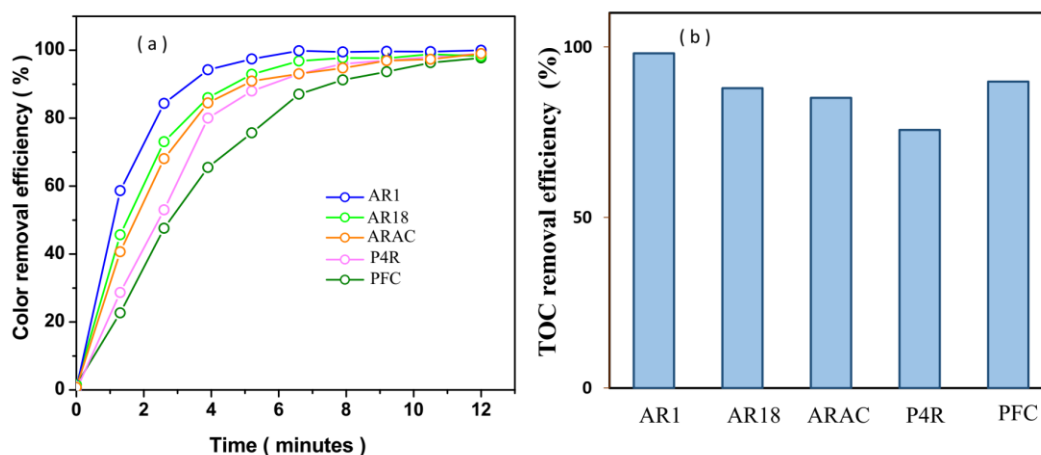


Figure 9. Application of PEF under the identified optimal conditions (0.05 M Na_2SO_4 and 0.5 mM Fe^{2+} , pH 3.0, 66.6 mA/cm^2 , 35 °C and each dye concentration of 300 mg/l) to decolorization of AR1, AR18, ARAC, P4R and PFC (a) decolorization efficiency and (b) TOC removal efficiency at 240 minutes.

4. CONCLUSION

This work was conducted on the study and application of the BDD/GDE cell for the decolorization of Acid Red 1 based on EF and PEF processes. The measurements were performed on the treatment of 100ml of 300 mg/l AR1 solution in 0.05 M Na_2SO_4 at pH 3.0 with 0.50 mM Fe^{2+} under applied current from 16.6 to 66.6 mA/cm^2 . The results indicated to the better performance of PEF method for color removal at 33.3 mA/cm^2 after 12 minutes of electrolysis, as it indicated 96.7% of the discoloration in PEF method and 95.2% of discoloration in the EF method. The degradation of the by-products generated during the reaction of AR1 and $\cdot\text{OH}$ was evaluated by solution TOC degradation. The evolution of OXL and OXM acids as degraded AR1 products by EF and PEF was also examined using HPLC. Results showed that the OXL and OXM acids were accumulated and destroyed by generated hydroxyl radicals. The slow reaction of Fe(III)-oxalate and Fe(III)-oxamate complexes with BDD($\cdot\text{OH}$) caused to slow degradation for long period and OXL and OXM acids were reduced to a final amount of 35.9 mg/l and 0.7 mg/l at 240 minutes. The evolution of SO_4^{2-} and NH_4^+ as released inorganic ions during the EF and PEF processes for the treatment of AR1 was determined by ion chromatography. The results of the time-course record of concentration of inorganic ions showed that the released SO_4^{2-} and NH_4^+ were completely released, accumulated and decayed by intermediates and reached to 98.2 mg/l and 42.5 mg/l for EF, and 98.2 mg/l and 6.5 mg/l for PEF at 240 minutes, respectively. The results demonstrated that the EF system was able to generate and accumulate a sufficient amount of H_2O_2 to adequately treat a solution with 100 mg/l TOC of AR1 by EF and PEF, and the higher rate of mineralization in PEF related to a synergistic effect in the generation of free radicals to destroy organic dyes and UVA light where the radicals contribute to the oxidation mechanism, which corresponds to dye elimination, and oxidation products are more quickly destroyed upon UVA light irradiation. Therefore, these findings show that the PEF process can be a

successful method to quickly destroy and mineralize azo dye-contaminated wastewater.

ACKNOWLEDGEMENT

The research is supported by: Scientific research project of Nanjing Polytechnic Institute (No. NJPI-2021-02).

References

1. S. Yang, X. Wan, K. Wei, W. Ma and Z. Wang, *Minerals Engineering*, 169 (2021) 106966.
2. H. Zhu, J. Zhu, Z. Zhang and R. Zhao, *The Journal of Physical Chemistry C*, 125 (2021) 26542.
3. L. Jia, Y. Yu, Z.-p. Li, S.-n. Qin, J.-r. Guo, Y.-q. Zhang, J.-c. Wang, J.-c. Zhang, B.-g. Fan and Y. Jin, *Bioresource Technology*, 332 (2021) 125086.
4. E. Rezaei-Seresht, A. Salimi and B. Mahdavi, *Pigment & Resin Technology*, 48 (2019) 84.
5. L.E. Gray Jr and J.S. Ostby, *Fundamental and Applied Toxicology*, 20 (1993) 177.
6. L. He, M.-X. Li, F. Chen, S.-S. Yang, J. Ding, L. Ding and N.-Q. Ren, *Journal of Hazardous Materials*, 417 (2021) 126113.
7. D. Ge, H. Yuan, J. Xiao and N. Zhu, *Science of The Total Environment*, 679 (2019) 298.
8. G. Li, S. Huang, N. Zhu, H. Yuan and D. Ge, *Journal of Hazardous Materials*, 403 (2021) 123981.
9. X. Wang, Y. Zhang, M. Luo, K. Xiao, Q. Wang, Y. Tian, W. Qiu, Y. Xiong, C. Zheng and H. Li, *Science of The Total Environment*, 763 (2021) 144616.
10. M. Wang, S. Yuan, B. Lv and D. He, *International Journal of Electrochemical Science*, 16 (2021) 210546.
11. N. Wächter, G.F. Pereira, R.C. Rocha-Filho, N. Bocchi and S.R. Biaggio, *International Journal of Electrochemical Science*, 10 (2015) 1361.
12. V. Rondán, B. Ramírez, S. Silva-Martínez, J. Hernández, M.K. Tiwari and A. Alvarez-Gallegos, *International Journal of Electrochemical Science*, 15 (2020) 52.
13. C. Flox, J.A. Garrido, R.M. Rodríguez, P.-L. Cabot, F. Centellas, C. Arias and E. Brillas, *Catalysis Today*, 129 (2007) 29.
14. E.J. Ruiz, C. Arias, E. Brillas, A. Hernández-Ramírez and J. Peralta-Hernández, *Chemosphere*, 82 (2011) 495.
15. H. Maleh, M. Alizadeh, F. Karimi, M. Baghayeri, L. Fu, J. Rouhi, C. Karaman, O. Karaman and R. Boukherroub, *Chemosphere*, (2021) 132928.
16. C. O'Neill, A. Lopez, S. Esteves, F. Hawkes, D. Hawkes and S. Wilcox, *Applied microbiology and biotechnology*, 53 (2000) 249.
17. S.-S. Yang, X.-L. Yu, M.-Q. Ding, L. He, G.-L. Cao, L. Zhao, Y. Tao, J.-W. Pang, S.-W. Bai and J. Ding, *Water Research*, 189 (2021) 116576.
18. M. Wang, C. Jiang, S. Zhang, X. Song, Y. Tang and H.-M. Cheng, *Nature chemistry*, 10 (2018) 667.
19. S. Thomas, S.V. Abraham, U.K. Aravind and C.T. Aravindakumar, *Environmental Science and Pollution Research*, 24 (2017) 24533.
20. Y. Orooji, B. Tanhaei, A. Ayati, S.H. Tabrizi, M. Alizadeh, F.F. Bamoharram, F. Karimi, S. Salmanpour, J. Rouhi and S. Afshar, *Chemosphere*, 281 (2021) 130795.
21. X. Zhang, Y. Tang, F. Zhang and C.S. Lee, *Advanced Energy Materials*, 6 (2016) 1502588.
22. N. Bensalah, A. Bedoui, S. Chellam and A. Abdel-Wahab, *CLEAN–Soil, Air, Water*, 41 (2013) 635.

23. A. Bedolla-Guzman, I. Sirés, A. Thiam, J.M. Peralta-Hernández, S. Gutiérrez-Granados and E. Brillas, *Electrochimica Acta*, 206 (2016) 307.
24. X. Florenza, A.M.S. Solano, F. Centellas, C.A. Martínez-Huitle, E. Brillas and S. Garcia-Segura, *Electrochimica Acta*, 142 (2014) 276.
25. J.M. Jabar and Y.A. Odusote, *Arabian Journal of Chemistry*, 13 (2020) 5417.
26. B.N. Zwane, B.O. Orimolade, B.A. Koiki, N. Mabuba, C. Gomri, E. Petit, V. Bonniol, G. Lesage, M. Rivallin and M. Cretin, *Water*, 13 (2021) 2772.
27. K. Bevziuk, A. Chebotarev, D. Snigur, Y. Bazel, M. Fizer and V. Sidey, *Journal of Molecular Structure*, 1144 (2017) 216.
28. H.M. Baker and K.F. Alzboon, *European Journal of Chemistry*, 6 (2015) 135.
29. M. Shukor, M.A. Syed, S. Raslan, K. Ithnin, N. Shamaan and M. Syed, *Bulletin of Environmental Science and Sustainable Management (e-ISSN 2716-5353)*, 1 (2013) 5.
30. M.F. Murrieta, I. Sirés, E. Brillas and J.L. Nava, *Chemosphere*, 246 (2020) 125697.
31. H.Y. Lee, X. Song, H. Park, M.-H. Baik and D. Lee, *Journal of the American Chemical Society*, 132 (2010) 12133.
32. A. El-Ghenymy, J.A. Garrido, F. Centellas, C. Arias, P.L. Cabot, R.M. Rodríguez and E. Brillas, *The Journal of Physical Chemistry A*, 116 (2012) 3404.
33. S. Garcia-Segura, Á.S. Lima, E.B. Cavalcanti and E. Brillas, *Electrochimica Acta*, 198 (2016) 268.
34. C. Ridruejo, F. Alcaide, G. Álvarez, E. Brillas and I. Sirés, *Journal of Electroanalytical Chemistry*, 808 (2018) 364.
35. E. Brillas and S. Garcia-Segura, *Water Conservation Science and Engineering*, 1 (2016) 83.
36. O. Scialdone, A. Galia, C. Gattuso, S. Sabatino and B. Schiavo, *Electrochimica Acta*, 182 (2015) 775.
37. F.C. Moreira, S. Garcia-Segura, V.J.P. Vilar, R.A.R. Boaventura and E. Brillas, *Applied Catalysis B: Environmental*, 142-143 (2013) 877.
38. A. El-Ghenymy, N. Oturan, M.A. Oturan, J.A. Garrido, P.L. Cabot, F. Centellas, R.M. Rodríguez and E. Brillas, *Chemical Engineering Journal*, 234 (2013) 115.
39. F. Martínez, G. Calleja, J. Melero and R. Molina, *Applied Catalysis B: Environmental*, 70 (2007) 452.
40. M. Ghahrchi, A. Rezaee and A. Adibzadeh, *Desalination and Water Treatment*, 211 (2021) 123.
41. J. Peralta-Hernández, C.A. Martínez-Huitle, J.L. Guzmán-Mar and A. Hernández-Ramírez, *Journal of Environmental Engineering and Management*, 19 (2009) 257.
42. C.M. Dominguez, N. Oturan, A. Romero, A. Santos and M.A. Oturan, *Chemosphere*, 202 (2018) 400.
43. M. Skoumal, R.M. Rodríguez, P.L. Cabot, F. Centellas, J.A. Garrido, C. Arias and E. Brillas, *Electrochimica Acta*, 54 (2009) 2077.
44. R. Salazar, S. Garcia-Segura, M. Ureta-Zañartu and E. Brillas, *Electrochimica acta*, 56 (2011) 6371.
45. A.A. Babaei, F. Ghanbari and R.J. Yengejeh, *Water Science and Technology*, 75 (2017) 1732.
46. J.-P. Simonin, *Chemical Engineering Journal*, 300 (2016) 254.
47. E. Brillas, *Journal of the Brazilian Chemical Society*, 25 (2014) 393-.
48. O. García, E. Isarain-Chávez, S. Garcia-Segura, E. Brillas and J.M. Peralta-Hernández, *Electrocatalysis*, 4 (2013) 224.
49. B. Garza-Campos, E. Brillas, A. Hernández-Ramírez, A. El-Ghenymy, J.L. Guzmán-Mar and E.J. Ruiz-Ruiz, *Journal of hazardous materials*, 319 (2016) 34.
50. E. Brillas, *Journal of the Mexican Chemical Society*, 58 (2014) 239.
51. S. Garcia-Segura, J.A. Garrido, R.M. Rodríguez, P.L. Cabot, F. Centellas, C. Arias and E. Brillas, *Water research*, 46 (2012) 2067.

52. L.C. Almeida, S. Garcia-Segura, C. Arias, N. Bocchi and E. Brillas, *Chemosphere*, 89 (2012) 751.
53. G.F. Pereira, A. El-Ghenymy, A. Thiam, C. Carlesi, K.I. Eguiluz, G.R. Salazar-Banda and E. Brillas, *Separation and Purification Technology*, 160 (2016) 145.
54. E.J. Ruiz, A. Hernández-Ramírez, J.M. Peralta-Hernández, C. Arias and E. Brillas, *Chemical Engineering Journal*, 171 (2011) 385.
55. C. Flox, P.-L. Cabot, F. Centellas, J.A. Garrido, R.M. Rodríguez, C. Arias and E. Brillas, *Applied Catalysis B: Environmental*, 75 (2007) 17.
56. E. Guinea, J.A. Garrido, R.M. Rodríguez, P.-L. Cabot, C. Arias, F. Centellas and E. Brillas, *Electrochimica Acta*, 55 (2010) 2101.

© 2022 The Authors. Published by ESG (www.electrochemsci.org). This article is an open access article distributed under the terms and conditions of the Creative Commons Attribution license (<http://creativecommons.org/licenses/by/4.0/>).